Ruthenium isotopes show the Chicxulub impactor was a carbonaceous-type asteroid

Mario Fischer-Gödde[1]*, Jonas Tusch[1], Steven Goderis[2], Alessandro Bragagni[3,4], Tanja Mohr-Westheide[5], Nils Messling[6], Bo-Magnus Elfers[7], Birger Schmitz[8], Wolf U. Reimold[9], Wolfgang D. Maier[10], Philippe Claeys[2], Christian Koeberl[11], François L. H. Tissot[12], Martin Bizzarro[13], Carsten Münker[1]

[1]Institut für Geologie und Mineralogie, University of Cologne, 50674 Cologne, Germany
[2]Archeology, Environmental Changes & Geo-Chemistry, Vrije Universiteit Brussel, 1050 Brussels, Belgium
[3]Department of Earth Sciences, University of Florence, Firenze 50121, Italy
[4]Institute of Marine Sciences, National Research Council, Bologna 40129, Italy
[5]Museum für Naturkunde, Leibniz-Institut für Evolutions- und Biodiversitätsforschung, 10115 Berlin, Germany
[6]Geochemistry and Isotope Geology Department, Geoscience Center, University of Göttingen, 37073 Göttingen, Germany
[7]Zentrallabor, Technical University Hamburg, 21073 Hamburg, Germany
[8]Astrogeobiology Laboratory, Lund University, SE-22100 Lund, Sweden
[9]Laboratório de Geocronologia e Geoquímica Isotópica, Instituto de Geociências, Universidade de Brasília, Campus Darcy Ribeiro, Asa Norte, CEP 70910-900, Brasília, DF, Brazil
[10]School of Earth & Ocean Sciences, Cardiff University, Cardiff CF10 3 AT, UK
[11]Department of Lithospheric Research, University of Vienna, A-1090 Vienna, Austria
[12]The Isotoparium, Division of Geological and Planetary Sciences, California Institute of Technology, Pasadena CA 91125, USA
[13]StarPlan – Center for Star and Planet Formation, GLOBE Institute, University of Copenhagen, Copenhagen, DK-1350, Denmark

*Corresponding author. Email: mfisch48@uni-koeln.de

An impact at Chicxulub occurred 66 million years ago, producing a global stratigraphic layer that marks the boundary between the Cretaceous and Paleogene eras. That layer contains elevated concentrations of platinum-group elements, including ruthenium. We measure ruthenium isotopes in samples taken from three Cretaceous-Paleogene boundary sites, five other impacts that occurred between 36 to 470 million years ago, and ancient 3.5 to 3.2 billion-year-old impact spherule layers. Our data indicate that the Chicxulub impactor was a carbonaceous-type asteroid, which had formed beyond the orbit of Jupiter. The other younger impact structures have isotopic signatures more consistent with siliceous-type asteroids, which formed closer to the Sun. The ancient spherule layer samples are consistent with impacts of carbonaceous-type asteroids during Earth's final stages of accretion.

Several mass extinction events occurred on Earth during the last 500 million years of its history, all within the Phanerozoic era, a geologic time period from 539 million years ago to the present (*1, 2*). The most recent mass extinction occurred simultaneously with the Cretaceous-Paleogene (K-Pg) geologic boundary, 66 million years ago (Ma), during which $\gtrsim$ 60 % of all species were extinguished (*3*). The geologic signature of the K-Pg boundary was produced by the impact on Earth of a >10 km diameter asteroid at Chicxulub, Mexico (*3, 4*). Samples taken from the K-Pg boundary layers have elevated concentrations of platinum group elements (PGE): iridium, ruthenium, osmium, rhodium, platinum and palladium (*5-7*), which are rare in Earth's crustal rocks (*8*). Meteorites, which are fragments of asteroids, have orders of magnitude higher PGE contents (*9*). The PGE enrichment of K-Pg boundary layer samples, and other terrestrial impact-related rocks and deposits, is interpreted as being derived from the extraterrestrial impactors.

Elevated PGE concentrations have been identified in many samples from globally distributed K-Pg boundary sites (*10-12*), indicating the fallout produced by the impact extended worldwide. The PGE data have been interpreted as indicating the impactor was an asteroid with composition similar to the class of meteorites known as chondrites (*13*). Further evidence for extraterrestrial material in the K-Pg boundary layer includes chromium (Cr) isotope data (*14, 15*) and the presence of a fossil meteorite fragment in a sample of the K-Pg boundary in the Pacific Ocean (*16*).

An alternative hypothesis for the origin of PGE in K-Pg boundary layer deposits is that they are derived from global ash fall originating from extensive volcanic eruptions in the Deccan Trap, India (*17*). However, the abundance ratios of PGEs in the K-Pg boundary differ from those in the Deccan Trap volcanic basalts (*18*); the K-Pg PGE relative abundances are more consistent with those of chondritic meteorites (*13*), not with Deccan basalts.

The abundance ratios of PGEs and osmium isotope compositions have been used to constrain the nature of the extraterrestrial impactors for Brent (*19*), Clearwater East (*20*), Morokweng (*21, 22*), Popigai (*23*) impact structures and ancient 3.5 to 3.2 Ga old impact spherule layers (*24-26*). This approach assumes that relative PGE abundances were not modified during the impact itself, during incorporation into the impact-generated host rocks, or by later processes affecting those rocks.

Ruthenium isotope constraints on extraterrestrial impactors

We investigate the nature of extraterrestrial impactors using the isotopic composition of ruthenium (Ru), a PGE. We chose Ru because it exhibits isotopic variations between different meteorite groups (*27-30*), which all differ from the terrestrial composition, so could serve as a genetic fingerprint for determining the source of the extraterrestrial component in impact rocks. For terrestrial impact rocks, the Ru isotopic signature of the impactor is expected to be preserved, even if inter-element PGE abundance ratios are modified during the impact or subsequent geologic processes (*13*).

If Ru in the K-Pg boundary layer and other terrestrial impact structures originate from extraterrestrial bodies, their Ru isotopic compositions will differ from Earth's, but be similar to those of the associated classes of meteorites. The Ru isotope signatures among meteorites scale with the heliocentric distance (distance from the Sun) at which their parent asteroids formed in the early Solar System (*30*). Two major classes of meteorites can be distinguished based on systematic differences in isotopic compositions of various elements (*31*): 1.) the carbonaceous (CC) meteorites comprising chondrites of Ivuna- (CI), Mighei- (CM), Ornans- (CO), Vigarano- (CV), Karoonda- (CK), Renazzo- (CR), High-iron- (CH), and Bencubbinit-types (CB), as well as isotopically associated iron meteorite groups (CC irons: IIC, IID, IIF, IIIF, IVB); 2.) the non-carbonaceous (NC) meteorites comprising ordinary- (OC), enstatite- (EC), and Rumuruti-type (RC) chondrites, as well as associated iron meteorite groups (NC irons: IAB, IIAB, IIAB, IIIE, IVA).

OCs are by far the most common type of stony meteorites arriving at Earth. OCs, ECs and RCs are fragments of siliceous (S-type) asteroids that formed in the inner Solar System, in the same region as the rocky planets (*31, 32*). The Ru isotope signatures of NC meteorites (OC, EC, RC and most NC irons) are less distinct from the Ru isotope composition of Earth (Fig. 1). In contrast, carbonaceous chondrite (CC) meteorites and isotopically associated iron meteorites (CC irons) are derived from carbonaceous (C-type) asteroids which formed at greater heliocentric distances, beyond the orbit of Jupiter (*31, 32*). The average Ru isotope compositions of CCs and CC irons are more distinct from Earth than OCs and ECs (Fig. 1). However, unlike other meteorite groups the CCs have large variations in between individual meteorites (Fig. 1), and CIs appear to be distinct from other CC groups (*30*).

Almost all meteorites that impact Earth are delivered from the current asteroid belt, located between the orbits of Mars and Jupiter, with CCs having migrated there due to scattering by the giant planets (*32*). Nevertheless, the difference in Ru isotope compositions with Earth follows the sequence EC<OC<CC, so distinguishes between asteroid material with C-type or S-type composition. Therefore, Ru can potentially be used to determine if an impactor originally formed in the inner or outer Solar System (*27-30*).

Ruthenium isotope measurements

We measured Ru isotopes to constrain the origins of the Chicxulub impactor, using samples taken from the K-Pg boundary (*33*). For comparison, we apply the same analysis to other Phanerozoic impact structures, ancient (3.5 to 3.2 Ga old) impact-related spherule layers, and two carbonaceous meteorites (CI and CV). Our samples were taken from widely separated K-Pg boundary sites from locations in Europe, to span a range of the Chicxulub ejecta layer. We used geologic sections collected from Denmark (Stevns Klint), Italy (Fonte D'Olio) and Spain (Caravaca). For the other Phanerozoic impacts, we used three drill core samples of impact melt rock from the Brent (Ontario, Canada), Clearwater East (Quebec, Canada) and Morokweng (South Africa) impact structures; surface impact melt rocks from Rochechouart (north-west Massif Central, France) and Popigai (Siberia, Russia) (*34, 35*). Three ancient impact spherule layer samples (BARB5_SL2, CT3-1_SL9, CT3-2_SL13) of the Barberton greenstone belt (South Africa) were taken from drill cores (core names: BARB5 & CT3, Table S1) (33). These spherule layers are dated 3.5 to 3.2 Ga and represent the oldest records of large asteroid impacts in the early Earth's history during the Archean era (*24-26*), a geologic time period from 4.0 to 2.5 Ga. Table S1 lists the sample locations and other detailed information (*33*). We also measured terrestrial standard samples (PGE-rich chromitite layer (UG2) from the Bushveld intrusion in South Africa), the CV meteorite Allende and the CI meteorite Orgueil.

All isotopic measurements used multi-collector inductively coupled plasma mass spectrometry (MC-ICPMS) (*33*). The resulting Ru isotopic compositions are listed in Table 1.

The differences between the Ru isotope compositions of meteorites and Earth are very small, so are conventionally reported in ε notation, which indicates the deviation in parts per 10,000 (0.01 % from a terrestrial isotopic standard (Table 1) and 'Materials and Methods' for details) (*33*). The uncorrected raw data, interference corrected and internally normalized data, and calculated ε values are provided in Data S1.

We find that all the impact-related samples have Ru isotopic compositions that are distinct from Earth and overlap those of meteorites (Fig. 1). A plot of ε^{102}Ru as a function of ε^{100}Ru (Fig. 2) shows that these variations are the same as observed for meteorites. We interpret this plot as indicating variable incorporation into Solar System bodies of cosmic dust enriched in Ru nuclides, produced by the slow neutron capture process (s-process) of stellar nucleosynthesis (*36*).

Origin of the Chicxulub impactor

All our K-Pg boundary layer samples exhibit indistinguishable and uniform Ru isotope compositions. The ε^{100}Ru values are distinct from the composition of Earth, ECs and OCs but consistent with the average composition of CCs (Fig. 1). This implies that the Chicxulub impactor was derived from the population of C-type asteroids that formed in the outer Solar System.

Although the ε^{100}Ru values of the K-Pg boundary layer samples are consistent with the average CC value (-0.88±0.12, 95 % conf., Table S3), they are well resolved different from those of the CI group (-0.31±0.13, 2 s.d., Table S4) (*33*). CI carbonaceous chondrites were interpreted to have similar composition to comets (*37*); if CI chondrites are a proxy for cometary matter, our Ru measurements exclude a previously proposed cometary origin of the Chicxulub impactor (*38*). A CI-like composition of the Chicxulub impactor has previously been excluded by Cr isotope data (*15*), inter-element PGE ratios (*13*), and the fossil meteorite in a K-Pg boundary drill core section (*16*).

We computed (*33*) the ε^{100}Ru values that would be measured for various mixtures between an average carbonaceous chondrite composition and the continental crust. The results (Fig. 3A) show that Ru isotope signatures are almost insensitive to contamination by terrestrial target rocks, because the Ru abundance in continental crust (0.34 ppb) (*8*) is orders of magnitude lower than the average for CCs (838 ppb) (*9*). Even minute amounts of extraterrestrial impactor material (<0.5 %) are sufficient to produce a ε^{100}Ru value that is indistinguishable from that of the impactor. This is consistent with our measurement of all K-Pg boundary samples having uniform Ru isotope signatures (Figs. 1 & 2). If the Chicxulub impactor had an average carbonaceous chondrite Ru composition, we calculate the average amount of extraterrestrial material in our K-Pg boundary layer samples is between 0.8 % at Fonte D'Olio (Italy) and 6.6 % at Stevns Klint (Denmark). This is lower than previous estimates but falls within the range determined from Cr isotopes (0.1 % to 20 %) *(15)* and PGE abundances (1.6 % to 21 %) (*5*).

The CC-like Ru isotope compositions we measure in the K-Pg boundary layer samples are consistent with evidence from Cr isotopes (*14, 15*) and chondritic PGE ratios (*13*), which were also interpreted as indicating a C-type asteroid as the Chicxulub impactor. Additionally, our Ru data exclude Deccan Trap volcanic eruptions as the origin of the elevated PGE concentrations within the K-Pg boundary (*17*), because any Ru derived from the eruptions would have terrestrial Ru isotope composition so would not match the Ru isotope signatures of CCs.

Phanerozoic and Archean impactor compositions

Unlike the Chicxulub impact, our samples from other terrestrial impact structures and Archean spherule layers have Ru isotope signatures distinct from average CCs (Fig. 1). The investigated Phanerozoic impact structures have ages of 36 to 470 Ma (*34, 35*) (Table S1), but exhibit uniform Ru isotope signatures that are consistent with OCs, CIs, COs, RCs and IVA iron meteorites. The OC-like ε^{100}Ru values of Popigai, Brent, Clearwater East, and Morokweng impact melt rocks are consistent with previous interpretation of their PGE ratios as indicating OC impactor compositions (*19-23*). OC meteorites are derived from S-type asteroids that formed in the inner Solar System (*31, 32*). The Clearwater East (460 to 470 Ma) and Brent (453 Ma) impacts occurred during a period (the Ordovician era) that had a higher flux of OC material to Earth than at present, due to the breakup of an S-type parent asteroid at 466 Ma (*39, 40*). We computed the same mixing model as above but assuming an OC-like impactor. The results (Fig. 3A) show the relative proportions of extraterrestrial material in each of these samples is 0.18 % for Popigai, 2.6 % for Brent, 3.1 % for Clearwater East, 4.3 % for Morokweng, and 0.57 % for Rochechouart.

The three Archean spherule layer samples from Barberton also have uniform Ru isotope compositions which overlap those of CIs, COs, OCs, RCs and IVA iron meteorites. However, Previous Cr isotope measurements of other Barberton spherule layers with similar ages (3.5 to 3.2 Ga) were consistent with a CC-like (CI, CM, CO, CV) impactor composition (*41*). The Cr constraints (*41*) in conjunction with the general isotopic distinctions between CC and NC meteorites (*31*) exclude NC meteorite-like impactor compositions like OCs, RCs and IVA irons. However, the Cr isotope data used different samples than our study, because BARB5 and CT3 drill core samples were not available at that time. Our Ru isotope measurements of impact spherule layer samples from the BARB5 and CT3 drill cores exclude the compositions of most carbonaceous meteorite groups, with only CIs and COs remaining viable impactor compositions (Fig. 1). The Barberton spherule layer samples have very high Ru concentrations (529 to 2737 ppb, Table S1) (*33*), with the CT3 samples (CT3-1_SL9, CT3-2_SL13) exceeding the average Ru concentration of carbonaceous chondrites (838 ppb, Table S4) (*33*). We calculated another mixing model for CI or CO impactors (Fig 3B) (*33*), which reproduces the high Ru concentrations in the Barberton spherule layers only for very high impactor contributions (>83 % for CI and >54 % for CO). Similarly high impactor contributions (>90 %) to other Barberton spherule samples were previously inferred from Cr isotopes and PGE abundances (*41, 42*). The very high impactor contents in these spherule layers have been interpreted as due to accumulation or reworking processes of the primary impact deposits and their inherent extraterrestrial components, e.g., by hydraulic fractionation of components of different sizes and densities during fall, and after deposition by waves and currents (*43*), or by condensation of PGE-rich alloys from the impact vapor plume (*26, 43*).

Summary and conclusions

Our Ru isotope measurements constrain the origin of the Chicxulub impactor, five Phanerozoic impactors and Archean spherule layers which lack an identifiable impact structure. For five of the six investigated Phanerozoic impact structures, we conclude that most of the impactors were derived from S-type asteroids that formed in the inner Solar System, with Ru isotope compositions and PGE inter-element ratios most similar to OCs. In contrast, the Chicxulub impactor which produced the K-Pg boundary (66 Ma) and the much older Archean spherule layers (3.5 to 3.2 Ga) were both derived from objects with CC-like composition, indicating an origin in the outer Solar System (*33. 31*). The Ru data for Chicxulub are inconsistent with a previous proposal that the impactor was a comet (*38*). For the Archean spherule layers, the CC-like composition could arise from C-type asteroid material that impacted during the final stages of Earth's accretion (*44*).

References

1. W. J. Foster, B. J. Allen, N. H. Kitzmann, J. Münchmeyer, T. Rettelbach, J. D. Witts, R. J. Whittle, E. Larina, M. E. Clapham, A. M. Dunhill, How predictable are mass extinction events? *Royal Society Open Science* **10**, 221507 (2023).

2. D. M. Raup, J. J. Sepkoski, Mass Extinctions in the Marine Fossil Record. *Science* **215**, 1501-1503 (1982).

3. P. Schulte, L. Alegret, I. Arenillas, J. A. Arz, P. J. Barton, P. R. Bown, T. J. Bralower, G. L. Christeson, P. Claeys, C. S. Cockell, G. S. Collins, A. Deutsch, T. J. Goldin, K. Goto, J. M. Grajales-Nishimura, R. A. F. Grieve, S. P. S. Gulick, K. R. Johnson, W. Kiessling, C. Koeberl, D. A. Kring, K. G. MacLeod, T. Matsui, J. Melosh, A. Montanari, J. V. Morgan, C. R. Neal, D. J. Nichols, R. D. Norris, E. Pierazzo, G. Ravizza, M. Rebolledo-Vieyra, W. U. Reimold, E. Robin, T. Salge, R. P. Speijer, A. R. Sweet, J. Urrutia-Fucugauchi, V. Vajda, M. T. Whalen, P. S. Willumsen, The Chicxulub Asteroid Impact and Mass Extinction at the Cretaceous-Paleogene Boundary. *Science* **327**, 1214-1218 (2010).

4. S. L. Lyons, A. T. Karp, T. J. Bralower, K. Grice, B. Schaefer, S. P. S. Gulick, J. V. Morgan, K. H. Freeman, Organic matter from the Chicxulub crater exacerbated the K–Pg impact winter. *Proceedings of the National Academy of Sciences* **117**, 25327-25334 (2020).

5. F. T. Kyte, Z. Zhou, J. T. Wasson, Siderophile-enriched sediments from the Cretaceous–Tertiary boundary. *Nature* **288**, 651-656 (1980).

6. L. W. Alvarez, W. Alvarez, F. Asaro, H. V. Michel, Extraterrestrial Cause for the Cretaceous-Tertiary Extinction. *Science* **208**, 1095-1108 (1980).

7. J. Smit, J. Hertogen, An extraterrestrial event at the Cretaceous–Tertiary boundary. *Nature* **285**, 198-200 (1980).

8. R. L. Rudnick, S. Gao, in *Treatise on Geochemistry,* H. D. Holland, K. K. Turekian, Eds. (Pergamon, Oxford, 2003), pp. 1-64.

9. J. M. D. Day, A. D. Brandon, R. J. Walker, Highly Siderophile Elements in Earth, Mars, the Moon, and Asteroids. *Reviews in Mineralogy and Geochemistry* **81**, 161-238 (2016).

10. S. Goderis, H. Sato, L. Ferrière, B. Schmitz, D. Burney, P. Kaskes, J. Vellekoop, A. Wittmann, T. Schulz, S. M. Chernonozhkin, P. Claeys, S. J. de Graaff, T. Déhais, N. J. de Winter, M. Elfman, J.-G. Feignon, A. Ishikawa, C. Koeberl, P. Kristiansson, C. R. Neal, J. D. Owens, M. Schmieder, M. Sinnesael, F. Vanhaecke, S. J. M. Van Malderen, T. J. Bralower, S. P. S. Gulick, D. A. Kring, C. M. Lowery, J. V. Morgan, J. Smit, M. T. Whalen, I.-I. E. Scientists, Globally distributed iridium layer preserved within the Chicxulub impact structure. *Science Advances* **7**, eabe3647 (2021).

11. B. Schmitz, Origin of microlayering in worldwide distributed Ir-rich marine Cretaceous/Tertiary boundary clays. *Geology* **16**, 1068-1072 (1988).

12. P. Claeys, W. Kiessling, W. Alvarez, in *Catastrophic events and mass extinctions: impacts and beyond,* C. Koeberl, K. G. MacLeod, Eds. (Geological Society of America, 2002), vol. 356, pp. 55-68.

13. S. Goderis, R. Tagle, J. Belza, J. Smit, A. Montanari, F. Vanhaecke, J. Erzinger, P. Claeys, Reevaluation of siderophile element abundances and ratios across the Cretaceous–Paleogene (K–Pg) boundary: Implications for the nature of the projectile. *Geochimica et Cosmochimica Acta* **120**, 417-446 (2013).

14. A. Shukolyukov, G. W. Lugmair, Isotopic Evidence for the Cretaceous-Tertiary Impactor and Its Type. *Science* **282**, 927-930 (1998).

15. A. Trinquier, J.-L. Birck, C. Jean Allègre, The nature of the KT impactor. A 54Cr reappraisal. *Earth and Planetary Science Letters* **241**, 780-788 (2006).

16. F. T. Kyte, A meteorite from the Cretaceous/Tertiary boundary. *Nature* **396**, 237-239 (1998).

17. C. B. Officer, C. L. Drake, The Cretaceous-Tertiary Transition. *Science* **219**, 1383-1390 (1983).

18. B. J. Peters, J. M. D. Day, A geochemical link between plume head and tail volcanism. *Geochemical Perspectives Letters* **5**, 29-34 (2017).

19. H. Palme, R. A. F. Grieve, R. Wolf, Identification of the projectile at the Brent crater, and further considerations of projectile types at terrestrial craters. *Geochimica et Cosmochimica Acta* **45**, 2417-2424 (1981).

20. I. McDonald, Clearwater East impact structure: A re-interpretation of the projectile type using new platinum-group element data from meteorites. *Meteoritics & Planetary Science* **37**, 459-464 (2002).

21. I. McDonald, M. A. G. Andreoli, R. J. Hart, M. Tredoux, Platinum-group elements in the Morokweng impact structure, South Africa: Evidence for the impact of a large ordinary chondrite projectile at the Jurassic-Cretaceous boundary11Associate editor: C. Koeberl. *Geochimica et Cosmochimica Acta* **65**, 299-309 (2001).

22. W. D. Maier, M. A. G. Andreoli, I. McDonald, M. D. Higgins, A. J. Boyce, A. Shukolyukov, G. W. Lugmair, L. D. Ashwal, P. Gräser, E. M. Ripley, R. J. Hart, Discovery of a 25-cm asteroid clast in the giant Morokweng impact crater, South Africa. *Nature* **441**, 203-206 (2006).

23. R. Tagle, P. Claeys, Comet or Asteroid Shower in the Late Eocene? *Science* **305**, 492 (2004).

24. S. Ozdemir, T. Schulz, D. van Acken, A. Luguet, W. U. Reimold, C. Koeberl, Meteoritic highly siderophile element and Re-Os isotope signatures of Archean spherule layers from the CT3 drill core, Barberton Greenstone Belt, South Africa. *Meteoritics & Planetary Science* **54**, 2203-2216 (2019).

25. T. Schulz, C. Koeberl, A. Luguet, D. van Acken, T. Mohr-Westheide, S. Ozdemir, W. U. Reimold, New constraints on the Paleoarchean meteorite bombardment of the Earth – Geochemistry and Re-Os isotope signatures of spherule layers in the BARB5 ICDP drill core from the Barberton Greenstone Belt, South Africa. *Geochimica et Cosmochimica Acta* **211**, 322-340 (2017).

26. T. Mohr-Westheide, W. U. Reimold, J. Fritz, C. Koeberl, T. Salge, A. Hofmann, R. T. Schmitt, Discovery of extraterrestrial component carrier phases in Archean spherule layers: Implications for estimation of Archean bolide sizes. *Geology* **43**, 299-302 (2015).

27. E. A. Worsham, C. Burkhardt, G. Budde, M. Fischer-Gödde, T. S. Kruijer, T. Kleine, Distinct evolution of the carbonaceous and non-carbonaceous reservoirs: Insights from Ru, Mo, and W isotopes. *Earth and Planetary Science Letters* **521**, 103-112 (2019).

28. K. R. Bermingham, E. A. Worsham, R. J. Walker, New insights into Mo and Ru isotope variation in the nebula and terrestrial planet accretionary genetics. *Earth and Planetary Science Letters* **487**, 221-229 (2018).

29. M. Fischer-Gödde, C. Burkhardt, T. S. Kruijer, T. Kleine, Ru isotope heterogeneity in the solar protoplanetary disk. *Geochimica et Cosmochimica Acta* **168**, 151-171 (2015).

30. M. Fischer-Gödde, T. Kleine, Ruthenium isotopic evidence for an inner Solar System origin of the late veneer. *Nature* **541**, 525-527 (2017).

31. T. S. Kruijer, C. Burkhardt, G. Budde, T. Kleine, Age of Jupiter inferred from the distinct genetics and formation times of meteorites. *Proceedings of the National Academy of Sciences* **114**, 6712-6716 (2017).

32. K. J. Walsh, A. Morbidelli, S. N. Raymond, D. P. O'Brien, A. M. Mandell, A low mass for Mars from Jupiter's early gas-driven migration. *Nature* **475**, 206-209 (2011).

33. Materials and methods are available as supplementary materials.

34. T. Kenkmann, The terrestrial impact crater record: A statistical analysis of morphologies, structures, ages, lithologies, and more. *Meteoritics & Planetary Science* **56**, 1024-1070 (2021).

35. M. Gottwald, T. Kenkmann, W. U. Reimold, *Terrestrial impact structures: the TanDEM-X atlas*. (Verlag Dr. Friedrich Pfeil, 2020).

36. M. R. Savina, A. M. Davis, C. E. Tripa, M. J. Pellin, R. Gallino, R. S. Lewis, S. Amari, Extinct technetium in silicon carbide stardust grains: implications for stellar nucleosynthesis. *Science* **303**, 649-652 (2004).

37. H. Campins, T. D. Swindle, Expected characteristics of cometary meteorites. *Meteoritics & Planetary Science* **33**, 1201-1211 (1998).

38. A. Siraj, A. Loeb, Breakup of a long-period comet as the origin of the dinosaur extinction. *Scientific Reports* **11**, 3803 (2021).

39. F. Terfelt, B. Schmitz, Asteroid break-ups and meteorite delivery to Earth the past 500 million years. *Proceedings of the National Academy of Sciences* **118**, e2020977118 (2021).

40. P. R. Heck, B. Schmitz, W. F. Bottke, S. S. Rout, N. T. Kita, A. Cronholm, C. Defouilloy, A. Dronov, F. Terfelt, Rare meteorites common in the Ordovician period. *Nature Astronomy* **1**, 0035 (2017).

41. F. T. Kyte, A. Shukolyukov, G. n. W. Lugmair, D. R. Lowe, G. R. Byerly, Early Archean spherule beds: Chromium isotopes confirm origin through multiple impacts of projectiles of carbonaceous chondrite type. *Geology* **31**, 283-286 (2003).

42. W. U. Reimold, C. Koeberl, S. Johnson, I. McDonald, in *Impacts and the Early Earth,* I. Gilmour, C. Koeberl, Eds. (Springer Berlin Heidelberg, Berlin, Heidelberg, 2000), pp. 117-180.

43. D. R. Lowe, G. Byerly, F. T. Kyte, A. Shukolyukov, F. Asaro, A. Krull, Spherule Beds 3.47–3.24 Billion Years Old in the Barberton Greenstone Belt, South Africa: A Record of Large Meteorite Impacts and Their Influence on Early Crustal and Biological Evolution. *Astrobiology* **3**, 7-48 (2003).

44. M. Fischer-Gödde, B.-M. Elfers, C. Münker, K. Szilas, W. D. Maier, N. Messling, T. Morishita, M. Van Kranendonk, H. Smithies, Ruthenium isotope vestige of Earth's pre-late-veneer mantle preserved in Archaean rocks. *Nature* **579**, 240-244 (2020).

45. J. H. Chen, D. A. Papanastassiou, G. J. Wasserburg, Ruthenium endemic isotope effects in chondrites and differentiated meteorites. *Geochimica et Cosmochimica Acta* **74**, 3851-3862 (2010).

46. N. Dauphas, A. M. Davis, B. Marty, L. Reisberg, The cosmic molybdenum-ruthenium isotope correlation. *Earth and Planetary Science Letters* **226**, 465-475 (2004).

47. M. McGregor, M. R. Dence, C. R. M. McFarlane, J. G. Spray, U–Pb geochronology of apatite and zircon from the Brent impact structure, Canada: a Late Ordovician Sandbian–Katian boundary event associated with L-Chondrite parent body disruption. *Contributions to Mineralogy and Petrology* **175**, 63 (2020).

48. G. Schmidt, Clues to the nature of the impacting bodies from platinum-group elements (rhenium and gold) in borehole samples from the Clearwater East crater (Canada) and the Boltysh impact crater (Ukraine). *Meteoritics & Planetary Science* **32**, 761-767 (1997).

49. R. Tagle, P. Claeys, An ordinary chondrite impactor for the Popigai crater, Siberia. *Geochimica et Cosmochimica Acta* **69**, 2877-2889 (2005).

50. R. Tagle, R. T. Schmitt, J. Erzinger, Identification of the projectile component in the impact structures Rochechouart, France and Sääksjärvi, Finland: Implications for the impactor population for the earth. *Geochimica et Cosmochimica Acta* **73**, 4891-4906 (2009).

51. H. A. Tornabene, C. D. Hilton, K. R. Bermingham, R. D. Ash, R. J. Walker, Genetics, age and crystallization history of group IIC iron meteorites. *Geochimica et Cosmochimica Acta* **288**, 36-50 (2020).

52. M. F. Horan, R. J. Walker, J. W. Morgan, J. N. Grossman, A. E. Rubin, Highly siderophile elements in chondrites. *Chemical Geology* **196**, 5-20 (2003).

53. M. Fischer-Gödde, H. Becker, F. Wombacher, Rhodium, gold and other highly siderophile element abundances in chondritic meteorites. *Geochimica et Cosmochimica Acta* **74**, 356-379 (2010).

Acknowledgments: We thank Frank Wombacher, Ralf Schmitt and Almut Katzemich for their help and support. We thank James Day, Honami Sato and another anonymous reviewer for constructive comments that improved the manuscript. **Funding:** M.F.-G. was supported by DFG grant number FI 1704/5-1 within the priority program SPP 1833 'Building a Habitable Earth'. C.M. was supported by the European Commission through ERC grant number 669666 'Infant Earth'. P.C. and S.G. were was supported by the Research Foundation Flanders (FWO), BELSPO-Desire and VUB Strategic Research Program. A.B. was supported by the research infrastructure ECORD participating in the ITINERIS project, EU – Next Generation EU Mission 4 "Education and Research" CUP B53C22002150006. W.U.R. was supported by the Brazilian Coordination for the Improvement of Higher Education Personnel, Coordenação de Aperfeiçoamento de Pessoal de Nível Superior – Brazil (CAPES) - Finance Code 001. **Author contributions:** Conceptualization: M.F.-G, S.G., A.B., T.M.-W., C.M. Data acquisition and analysis: M.F.-G., J.T., N.M., B.-M.E. Interpretation, modelling and visualization: M.F.-G. Writing: M.F.-G. with contributions from all co-authors. **Competing interests:** The authors declare no competing interests. **Data and materials availability:** Samples were obtained from the locations and sources listed in table S1 and are archived for further study; details are given in the supplementary material. All data shown in figures or used for modelling are listed in tables S1-S4. Our Ru isotope measurements (raw, corrected and normalized) are provided in Data S1.

Supplementary Materials

Materials and Methods

Tables S1 to S4

References (*45-53*)

Data S1

Figure 1: ε^{100}Ru measurements terrestrial samples and meteorites. From top to bottom, the data are for K-Pg boundary sites, Phanerozoic impact structures, Archean spherule layers, CC meteorites (divided into types), EC meteorites, OC meteorites, Rumuruti-type meteorites, CC-like and NC-like iron meteorites (divided into groups). Vertical colored lines indicate the average values of ECs (green, ε^{100}Ru = –0.08±0.04, 95 % conf.), OCs (red, ε^{100}Ru = –0.29±0.03, 95 % conf.), CCs (blue, ε^{100}Ru = –0.88±0.12, 95 % conf.), and Earth's mantle (*44*) (black, ε^{100}Ru = 0.00±0.02, 95 % conf.), with shaded regions indicating their 95 % confidence intervals. For CC iron meteorites the calculated average composition is shown including groups IIC, IID, IIF, IIIF, IVB and Chinga (see Table S3 for details) (*33*). For ECs and OCs, white open symbols indicate individual meteorites and black solid symbols are their averages. All plotted terrestrial and meteorite data are listed in Tables 1 and S3 respectively; error bars reflect either 95 % confidence interval or 2 s.d. uncertainties as indicated in Tables 1 and S3 (*33*).

Figure 2: ε^{102}Ru as a function of ε^{100}Ru. Data for the same terrestrial samples as in Fig. 1 (see legend) are compared to averages of each of the meteorite classes (solid symbols) except CIs, which are plotted individually (open circles) because they are distinct from other CCs in Fig. 1. The solid black lines indicate the Ru isotope composition of Earth's crust, ε^{102}Ru ≡ 0 and ε^{100}Ru ≡ 0. The dashed line is our mixing model (*33*) between Earth's composition and a nucleosynthetic component (s-process) (see 'Materials and Methods' for details) (*33*). Solid black arrows indicate directions of excess and deficit in s-process component. Data are listed in Tables 1 and S3. Error bars reflect 95 % confidence interval or 2 s.d. uncertainties as indicated in Tables 1 and S3.

Figure 3: Ruthenium mixing models. Dashed lines indicate the calculated ε^{100}Ru, as a function of Ru abundance, for model compositions consisting of a mixture between Earth's continental crust (black square) and potential meteorite impactor compositions, in various proportions (labeled crosses). Color shaded regions indicate minimum and maximum calculated ε^{100}Ru (curved solid black lines) based on the uncertainties of the meteorite impactor compositions as detailed below. Horizontal solid black lines indicate the Ru isotope composition of Earth's crust, ε^{100}Ru ≡ 0 (0.34 ppb Ru). (**A**) Models assuming the impactor composition was (blue) the average CCs (ε^{100}Ru = –0.88±0.12 (95 % conf.) and 838 ppb Ru, black circle) or (red) average OCs (ε^{100}Ru = –0.29±0.03 (95 % conf.) and 818 ppb Ru, black diamond). Data for the K-Pg boundary samples (blue circles) are consistent with the CC mixture model in proportions of 1 to 10%. The other Phanerozoic impact samples (colored diamonds, see legend) are closer to the OC mixture model. (**B**) Models assuming impactor compositions matching (cyan) CIs (ε^{100}Ru = –0.31±0.13 (2 s.d.) and 637.4 ppb Ru, empty blue circle) or (purple) COs (ε^{100}Ru = –0.36±0.13 (2 s.d.) and 981 ppb Ru, empty purple circle). Plotted measurements are listed in Tables 1 and S4 and the parameters of each model are given in Table S4. Uncertainties on the Ru abundances are negligible (see 'Materials and Methods' for details about the mixing calculations) (*33*). In all cases, we find that even a small contribution (> 0.5%) of impactor material causes the measured ε^{100}Ru to be close to the meteorite value.

Table 1: Ruthenium isotope measurements. Isotope data are listed for five ruthenium isotopes, measured from the samples of the K-Pg boundary layer, other Phanerozoic impact structures, Archean spherule layers, two meteorites, and a terrestrial reference sample UG2 chromitite. n is the number of analyses of the same sample solution. Ruthenium isotope data have been internally normalized to $^{99}Ru/^{101}Ru$ and are expressed in ε notation as deviations from the Alfa Aesar Ru standard solution (*33*). Uncertainties for all samples are expressed as twice the standard deviation (2 s.d.) of repeated measurements calculated for the average for reference sample UG2 (UG2_average), from 11 individual analyses of 2 replicate digestions ('Materials and Methods', Table S2) (*33*).

Sample	**n**	**$\varepsilon^{96}Ru$**	**$\varepsilon^{98}Ru$**	**$\varepsilon^{100}Ru$**	**$\varepsilon^{102}Ru$**	**$\varepsilon^{104}Ru$**
K-Pg boundary layer:						
Caravaca	1	-0.0 ± 0.27	2.29 ± 0.46	-0.94 ± 0.11	-0.36 ± 0.15	0.18 ± 0.25
Fonte D'Olio	13	0.25 ± 0.27	0.07 ± 0.46	-1.02 ± 0.11	-0.43 ± 0.15	-0.01 ± 0.25
Stevns Klint-1	2	0.68 ± 0.27	0.58 ± 0.46	-1.02 ± 0.11	-0.35 ± 0.15	0.17 ± 0.25
Stevns Klint-2	1	0.07 ± 0.27	0.92 ± 0.46	-0.98 ± 0.11	-0.44 ± 0.15	0.09 ± 0.25
Stevns Klint-3	1	0.38 ± 0.27	1.41 ± 0.46	-0.95 ± 0.11	-0.45 ± 0.15	-0.12 ± 0.25
Phanerozoic impact structures:						
Popigai	1	0.52 ± 0.27	1.01 ± 0.46	-0.36 ± 0.11	-0.19 ± 0.15	-0.06 ± 0.25
Morokweng	5	0.14 ± 0.27	0.66 ± 0.46	-0.36 ± 0.11	-0.14 ± 0.15	0.04 ± 0.25
Rochechouart	3	0.20 ± 0.27	0.43 ± 0.46	-0.40 ± 0.11	-0.20 ± 0.15	-0.07 ± 0.25
Brent	2	0.15 ± 0.27	1.43 ± 0.46	-0.35 ± 0.11	-0.09 ± 0.15	-0.08 ± 0.25
Clearwater East	2	0.26 ± 0.27	0.29 ± 0.46	-0.37 ± 0.11	-0.26 ± 0.15	-0.08 ± 0.25
Archean impact spherule layers:						
BARB5_SL2	1	0.40 ± 0.27	0.03 ± 0.46	-0.33 ± 0.11	-0.16 ± 0.15	-0.01 ± 0.25
CT3-1_SL9	7	0.12 ± 0.27	0.27 ± 0.46	-0.27 ± 0.11	-0.16 ± 0.15	-0.04 ± 0.25
CT3-2_SL13	8	0.09 ± 0.27	0.10 ± 0.46	-0.30 ± 0.11	-0.12 ± 0.15	0.05 ± 0.25
Terrestrial reference samples:						
UG2_1	7	-0.09 ± 0.27	0.11 ± 0.46	0.01 ± 0.11	-0.06 ± 0.15	-0.11 ± 0.25
UG2_2	4	-0.12 ± 0.27	-0.12 ± 0.46	0.01 ± 0.11	0.03 ± 0.15	-0.11 ± 0.25
UG2_average	11	-0.10 ± 0.27	0.03 ± 0.46	0.01 ± 0.11	-0.02 ± 0.15	-0.11 ± 0.25
Meteorites:						
Allende (CV3)	1	0.52 ± 0.27	0.53 ± 0.46	-0.73 ± 0.11	-0.25± 0.15	0.21± 0.25
Orgueil (CI1)	1	1.52 ± 0.27	0.99 ± 0.46	-0.38 ± 0.11	-0.18± 0.15	0.01± 0.25

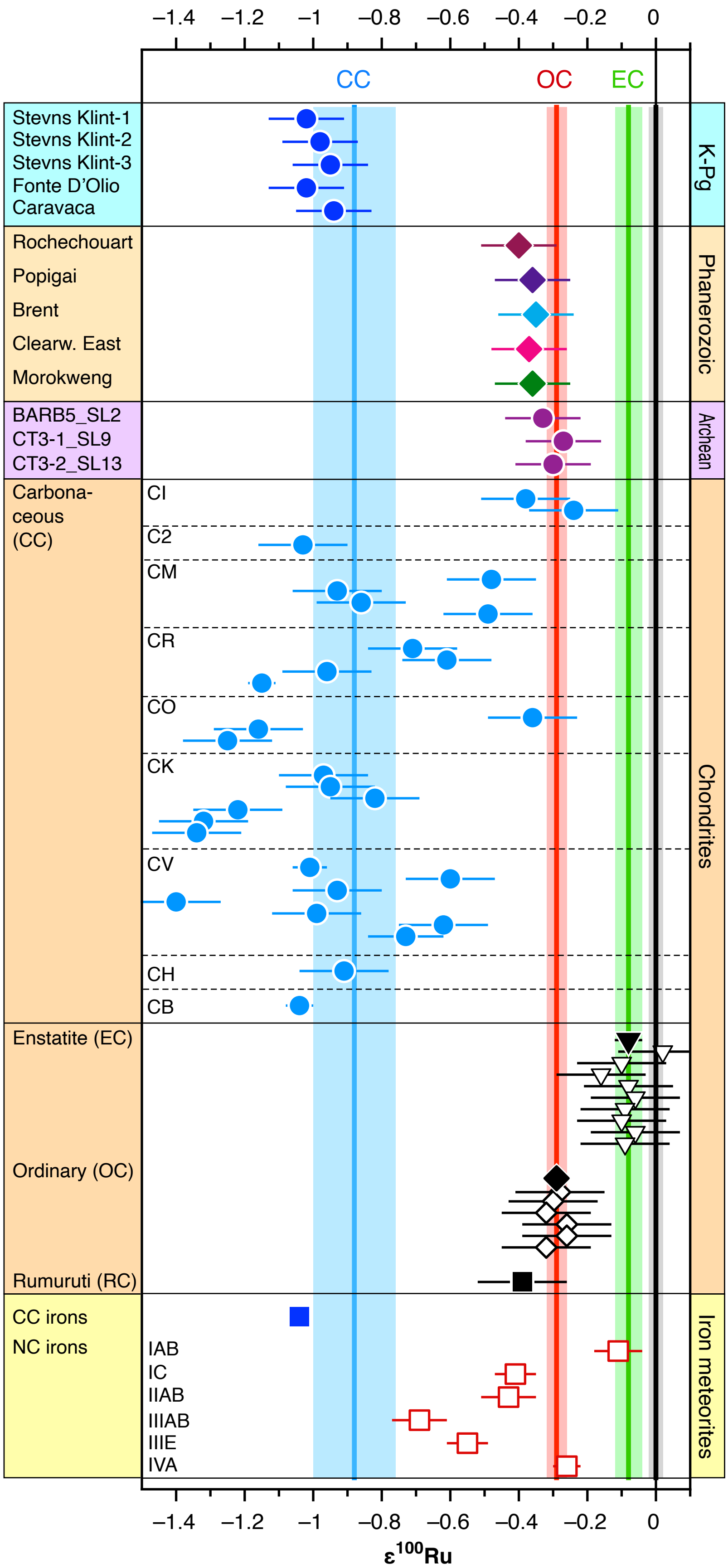

CC
OC
EC
Stevns Klint-1
Stevns Klint-2
Stevns Klint-3
Fonte D'Olio
Caravaca
K-Pg
Rochechouart
Popigai
Brent
Clearw. East
Morokweng
Phanerozoic
BARB5_SL2
CT3-1_SL9
CT3-2_SL13
Archean
Carbona-ceous (CC)
CI
C2
CM
CR
CO
CK
CV
CH
CB
Chondrites
Enstatite (EC)
Ordinary (OC)
Rumuruti (RC)
CC irons
NC irons
IAB
IC
IIAB
IIIAB
IIIE
IVA
Iron meteorites
−1.4 −1.2 −1 −0.8 −0.6 −0.4 −0.2 0
ε100Ru

490 **Figure 1**

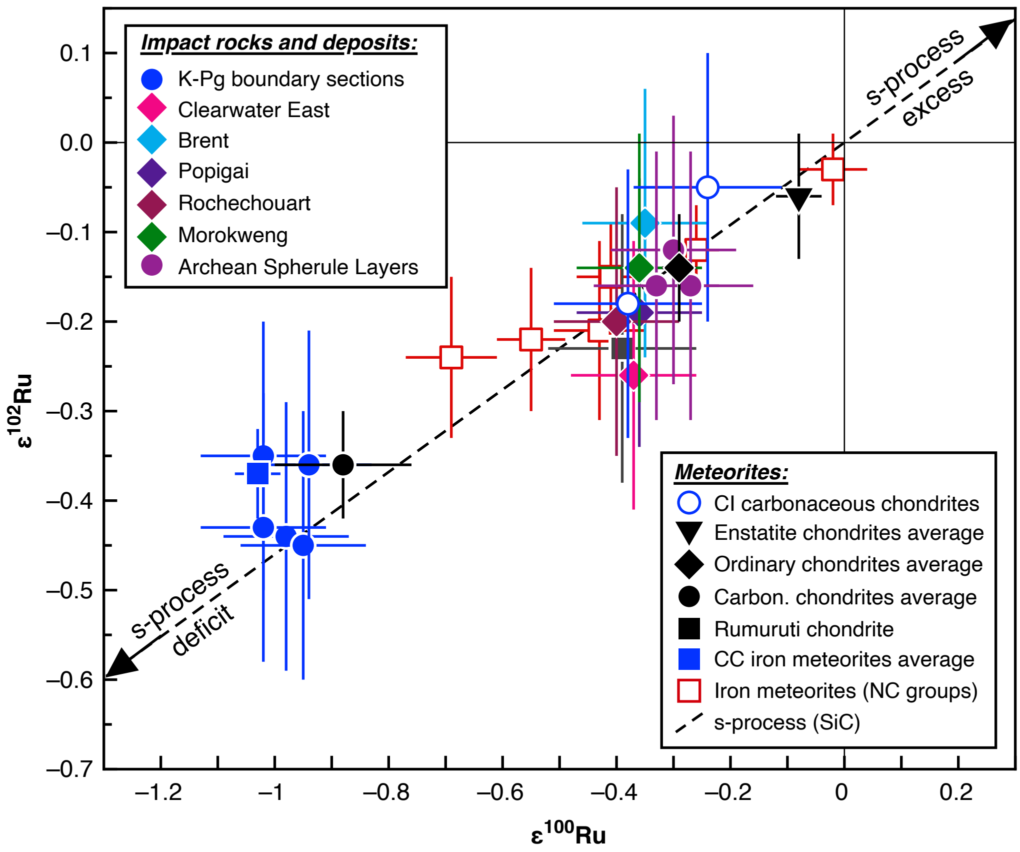
Impact rocks and deposits:
K-Pg boundary sections
Clearwater East
Brent
Popigai
Rochechouart
Morokweng
Archean Spherule Layers
Meteorites:
CI carbonaceous chondrites
Enstatite chondrites average
Ordinary chondrites average
Carbon. chondrites average
Rumuruti chondrite
CC iron meteorites average
Iron meteorites (NC groups)
s-process (SiC)
s-process excess
s-process deficit
ε102Ru
ε100Ru
0.1
0.0
–0.1
–0.2
–0.3
–0.4
–0.5
–0.6
–0.7
–1.2
–1
–0.8
–0.6
–0.4
–0.2
0
0.2

Figure 2

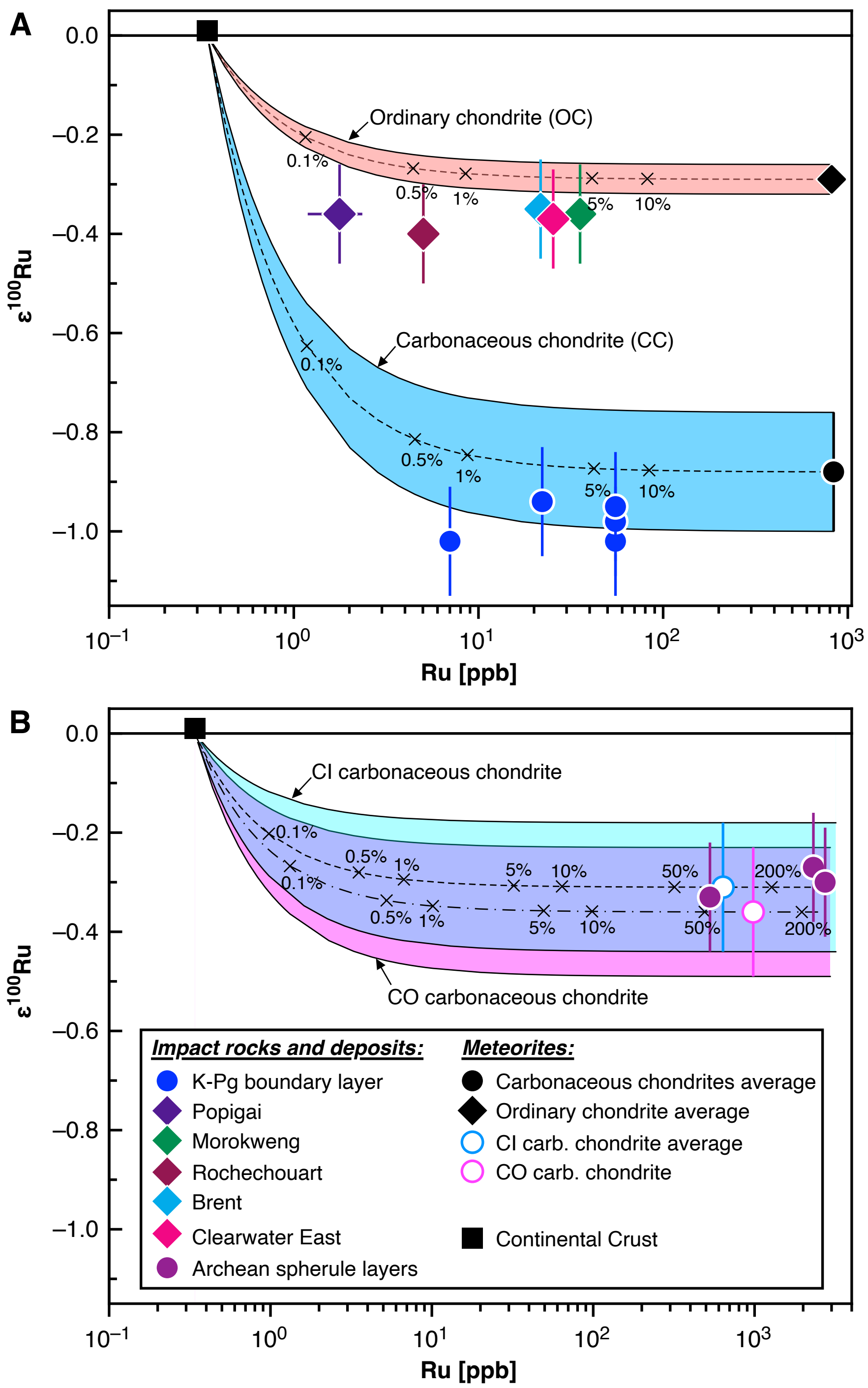
A
B
0.0
−0.2
−0.4
−0.6
−0.8
−1.0
ε100Ru
Ru [ppb]
10−1
10^0
10^1
10^2
10^3
Ordinary chondrite (OC)
Carbonaceous chondrite (CC)
0.1%
0.5%
1%
5%
10%
CI carbonaceous chondrite
CO carbonaceous chondrite
50%
200%
Impact rocks and deposits:
K-Pg boundary layer
Popigai
Morokweng
Rochechouart
Brent
Clearwater East
Archean spherule layers
Meteorites:
Carbonaceous chondrites average
Ordinary chondrite average
CI carb. chondrite average
CO carb. chondrite
Continental Crust

Figure 3